River Flow 2010 - Dittrich, Koll, Aberle & Geisenhainer (eds) - © 2010 Bundesanstalt für Wasserbau ISBN 978-3-939230-00-7

Influence of vegetation to boundary shear stress in open channel for overbank flow

B. Terrier, S. Robinson & K. Shiono
Department of Civil and Building Engineering, Loughborough University, Loughborough, England

A. Paquier
Hydrology-Hydraulics Research Unit, Cemagref, Lyon, France

T. Ishigaki
Engineering Department of Civil, Environmental and Applied System Engineering, Kansai University, Japan

ABSTRACT: In rivers, flooding can be attributed to the effects of increased flow resistance due to riparian vegetation. Simply removing vegetation from river banks cannot be considered as a solution to aid flood mitigation, because vegetation plays a vital role in river environment. The flow structure in a compound channel with vegetation along edge of river bank is still not well understood. To better apprehend the influence of flow resistance of such vegetation to flow structure and boundary shear stress, laboratory experiments were carried out at Loughborough University.The experiments were conducted in a 12 m long, 0.306 m wide compound channel. The channel had a single line of emergent 3 mm diameter rods with 35 mm diameter brush bristles along the edge of the floodplain. The rods were spaced at rod distance to diameter ratios of L/d=8 and L/d=16. These ratios are compatible with those of trees in the River Thames. Boundary shear stress was measured using a Preston tube and velocity using a Pitot tube. The velocity distribution showed velocity dip caused by the presence of brushes. The boundary shear stress significantly decreased when compared with that of without brushes. The drag force of brushes was estimated from the force balance using weight component and boundary shear force. The drag force increases almost linearly with water depth. Stage discharge curves exhibited unexpected behaviour from other researcher findings (Sun and Shiono 2009).

Keywords: Compound channel, vegetation, boundary shear stress, drag force

1 INTRODUCTION AND AIMS

Observations of river banks reveal that one-line vegetation growing along the edge of floodplain is a common arrangement. Such vegetation may be trees or bushes of different kinds and may be spaced in different ways. A single line of riparian vegetation may be used for bank stabilisation, to promote environmental diversity or for landscape amenity purposes (Hubble et al., 2009). The impacts of such arrangements on the boundary shear stress and flow structure of a compound channel, however, have been little studied in literature.

Pasche & Rouvre (1985) conducted experiments in a compound channel with vegetated floodplain, measuring velocity with an LDV and boundary shear stress with a Preston tube. Coherent structures were observed in the flow, reflecting the intensive momentum exchange taking place between the roughened floodplain and the main channel.

In Nepf (1999), Nepf highlighted the impact of the wake structures on the flow resistance of arrays of cylinders set up in different configurations. For cylinders in tandem, for example, the rod distance to diameter ratio L/d is a determining parameter in the suppression of the drag coefficient on the downstream cylinder, due to the wakes generated by the upstream cylinder.

Sun and Shiono (2009) carried out experiments with one-line of rods placed on the edge of floodplain. The flow structures resulting from the line of rods were totally different compared to that of a standard compound channel without rods. The velocity, discharge and boundary shear stress in the rod cases were considerably reduced compared to those in the no rod cases. Sun and Shiono (2009) used smooth wooden rods in their experiments and investigated two rod densities of approximately L/d=4.4 and 13.3.

The main aim of this paper is to investigate the boundary shear stress and flow structures in compound channels with one-line emergent rods with

bristles along the floodplain edge. The impacts of such vegetative structures on the stage discharge relationship, velocity distribution and boundary shear stress distributions are first presented. The evolution of drag force with relative depth and vegetation density is also examined.

2 EXPERIMENTAL METHODOLOGY

2.1 *Physical modeling of riparian vegetation*

An attempt was made to physically model vegetation with foliage along the floodplain. For that purpose, a series of test tube brushes from Fisher Scientific (code BUR-610-030G) with 3 mm diameter steel tube and 35 mm brush strand diameter, as shown in Figure 1, were lined along the floodplain edge to represent trees. The effective frontal area percentage of the brush was estimated by analyzing detailed photographs and is approximately 72%.

Each brush was prepared for the experiments by cutting the cotton end with wire cutters to obtain a constant density along the length of the brush. The final brushes were 50 mm high.

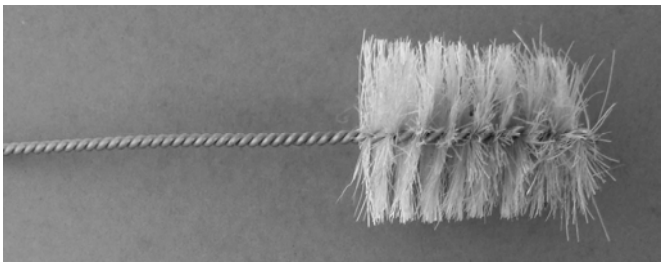

Figure 1. Brush

In order to adopt pertinent rod spacings, guidelines on planting trees found in literature were first studied to define applicable spacing ratios of rods. Spacings between 8 to 16 times the diameter of rods were found to be representative (Sun and Shiono, 2009; Terrier, 2010).

In addition, tree spacings were also surveyed along the floodplain of a stretch of the river Thames. The frequency diagram shown in Figure 2 presents the results of the survey.

Spacing ratios of L/d=8.0 and 16.0 were used to investigate the effects of vegetative density on the flow. The applicability of these spacing ratios was therefore confirmed via literature review and collection in field studies.

It is important to note that these spacing ratios are greater than the critical spacing ratios of 3.5~3.8 described in Zdravkovitch (1977), beyond which periodic vortex shedding is observed behind cylinders aligned in tandem.

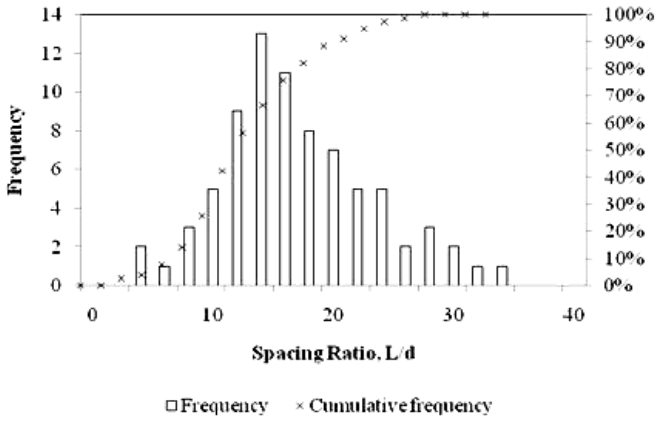

Figure 2. Vegetation survey along the River Thames

2.2 *Experimental methodology*

The measurements were conducted in a 12 m long Perspex tilting flume in the hydraulic laboratory at Loughborough University. Figure 3 illustrates the trapezoidal cross-section shape of the flume. The total width B of the flume was 0.306 m, the floodplain width B_{fp} was 0.150 m and the side slope s was 1. The flume bed slope (S_0) was set to be 0.001. The flow rate (Q) was measured by weighing the outlet water mass per unit time. The water depth was measured by a digital point gauge.

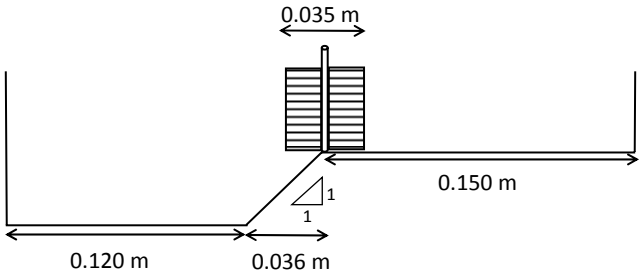

Figure 3. Compound channel cross-section at the brush

To minimize the effects of inlet turbulence on the flow development, a 0.1 m long Kraft honeycomb with uniform hexagonal holes was placed at the inlet to straighten the flow and a 0.25 m long float foam plate was fixed to the honeycomb to avoid the propagation of waves in the water surface downstream.

Quasi-uniform flow conditions were achieved by ensuring that the average water surface slope was parallel to the bed slope. In addition, detailed measurements of mean velocity were performed with a 2.2 mm diameter Pitot tube at the measuring sections and at approximately one meter upstream and downstream of the measuring section to verify the uniformity of the flow. The discrepancy between the mean velocity measured at these different sections was below 5% for all the

measured data points, hence providing confidence that the flow was quasi-uniform. The recording time for the Pitot tube was set to 1 min as this ensured that the measurements had converged.

Discharges were also calculated by integrating the velocity measured with the Pitot tube. The calculated discharges were then compared with the measured discharges. Errors were typically less than 5%, thereby ensuring some consistency in the measurements.

Boundary shear stress τ_B was measured using a Preston tube. The diameters of the static and dynamic pressure pipes of the Preston tube used in this study are 3.00 mm and 2.72 mm respectively. Patel's method was used (Patel, 1965). The recording time for the Preston tube was set to 3 min as this ensured convergence in the measurements.

2.3 *Summary of experiments*

In total, nine cases were investigated. Three no rod cases (Sa, Sb and Sc) provided reference cases. For a further six cases, rods with bristles were used (B8a, B8b and B8c) and (B16a, B16b and B16c) with spacing ratios of 8.0 and 16.0 respectively. The experiments for each rod density were conducted for three relative water depths (ratio between the floodplain water depth to the main channel water depth). The summary of the experiments carried out is given in Table 1.

Table 1. Summary of the Investigated Flow Cases

Flow case	Flow rate (m^3/s)	Relative depth	Reynolds number	Spacing ratio (L/d)
Sa	0.00220	0.24	23163	N/A
Sb	0.00352	0.37	35218	N/A
Sc	0.00543	0.50	50569	N/A
B8a	0.00183	0.25	12850	8.0
B8b	0.00225	0.35	17040	8.0
B8c	0.00330	0.51	25825	8.0
B16a	0.00178	0.25	13228	16.0
B16b	0.00210	0.35	15946	16.0
B16c	0.00273	0.51	22567	16.0

3 RESULTS

3.1 *Stage discharge*

Figure 4 presents the stage discharge curves for all nine cases. As expected, the channel discharge is seen to increase as the flow depth increases and the brushes provide a drop in total discharge compared to the no rod case. For all cases, the brushes significantly decrease the channel's total discharge in the compound channel when compared to no rod scenarios, by up to 50% for case B16c. The flow reduction due to the brushes increases notably with relative depth.

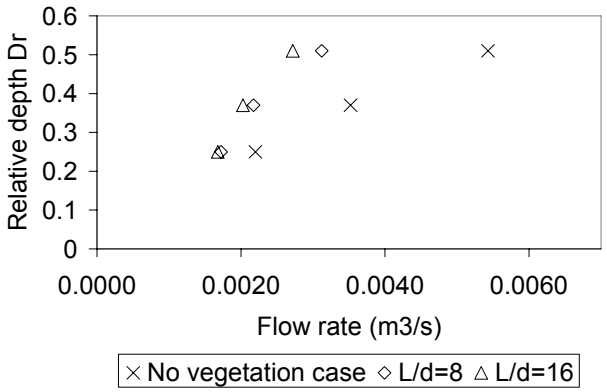

Figure 4. Stage discharge for the no vegetation and brush cases

Interestingly, the increase in vegetative density along the floodplain edge leads to a greater discharge for all channel stages when compared to the less dense vegetation. It had been expected that increasing the brush density (L/d decreasing) would lead to an increase in the chances of flooding, as was the case with the smooth rod cases presented in Sun and Shiono (2009). However, these results suggest that there is a threshold at which closer spacing of brushes can result in an increase in discharge, thereby reducing flooding effects.

Figure 5 gives a breakdown of the percentage of total discharge carried by the main channel and the floodplain. The discharge distribution is derived by integrating the depth-averaged velocities over the main channel and floodplain areas. In the no rod case, the floodplain carries a greater proportion of the total flow. As relative depth increases towards unity, the percentage of discharge in each section of the channel tends towards 51% and 49% for the main channel and floodplain respectively.

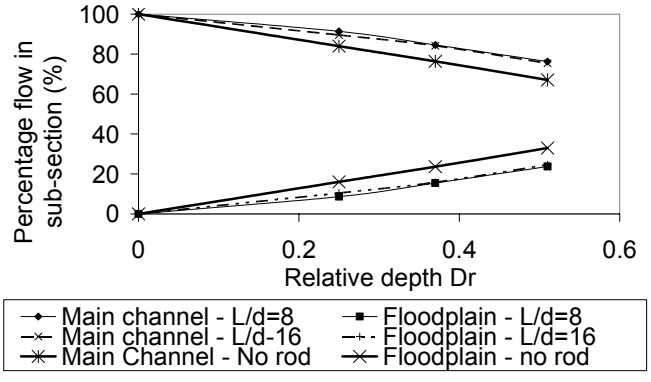

Figure 5. Discharge distribution for the brush cases

The Manning's n values were calculated using Equation 1.

$$n = \frac{R^{2/3} S_0^{1/2}}{U_m} \quad (1)$$

R is the hydraulic radius and U_m is the measured bulk velocity. Figure 6 gives the Manning's n values for the different cases.

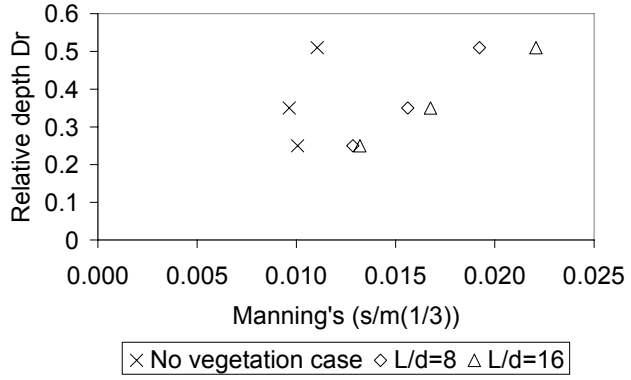

Figure 6. Mean calculated Manning's values

The brushes have for effect to increase significantly the Manning's n values, as they are comprised between 0.013 and 0.022. The L/d=8 cases have lower Manning's n values compared to the L/d=16cases, correlating the results of the stage discharge presented above, as should be.

3.2 *Velocity distributions*

The depth-averaged velocity $U_d(y)$ at a position y was calculated using Equation 2.

$$U_d(y) = \frac{1}{H(y)} \int_0^{H(y)} U(y)dz \quad (2)$$

Where $H(y)$ is the water depth at the position y. Figures 7 to 9 give the depth-averaged velocity distributions for the no rod cases (Cases Sa, Sb and Sc), the L/d=8 cases (Cases B8a, B8b and B8c) and the L/d=16 cases (Cases B16a, B16b and B16c) respectively. The maximum velocities are suppressed further as flow depth increases, with it being pushed closer to the boundary wall with increasing flow depth in the main. The velocity in the brush area appears more affected by the smaller water depths as vegetation density is changed.

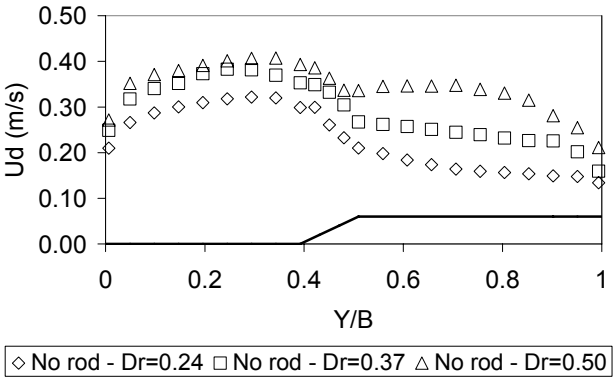

Figure 7. Depth-averaged velocity distribution for the no rod cases

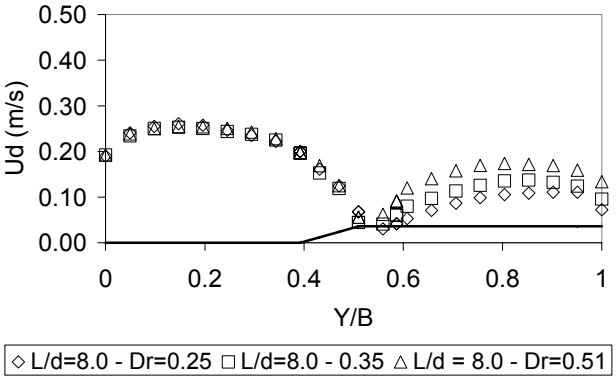

Figure 8. Depth-averaged velocity distribution for the brush cases with L/d=8 (Cases B8)

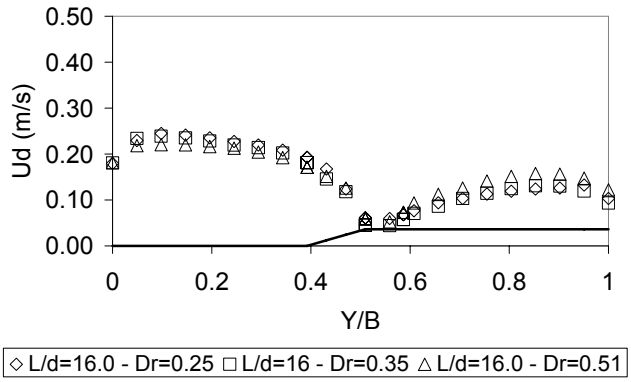

Figure 9. Depth-averaged velocity distribution for the brush cases with L/d=16 (Cases B16)

Cases B8 (Figure 8) indicates a larger discharge through the main channel than for Cases B16, and generally shows an increase in the floodplain area. At the point of vegetation, the velocity is slightly smaller for the denser vegetation, which is to be expected. For each case, the velocity in the main channel is slightly greater at lower flow depths whereas in the floodplain the greatest velocity occurs for the larger flow depths.

Although the brushes have a clear detrimental effect on the water levels from an engineering viewpoint, they also contribute to lower the velocities.

3.3 *Boundary shear stress*

The results of bed shear stress measurements are presented in Figures 10 to 12 for the no rod case, the L/d=8 cases and the L/d=16 case.

The lateral distributions of boundary shear stress follow the distributions of depth-averaged velocity. For both vegetative densities, the boundary shear stress distributions in the main channel are similar for all relative depths. On the floodplain, the larger relative depths provide a larger boundary shear stress with the maximum moving closer to the boundary wall with smaller relative depths, as was the case with the depth-averaged velocity distributions.

The differences in the magnitude of boundary shear stress between cases B8 and B16 are more significant in the floodplain than in the main channel. These differences increase with relative depths.

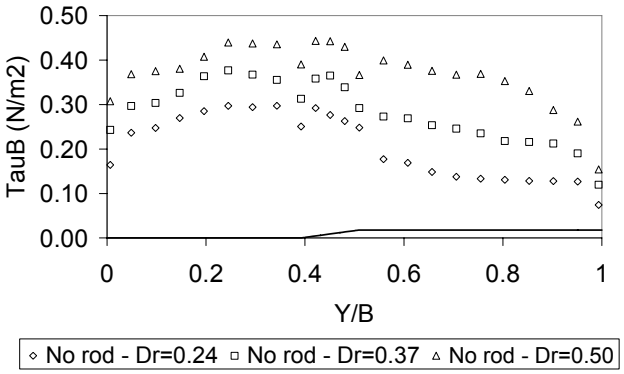

Figure 10. Boundary shear stress distribution for the no rod case

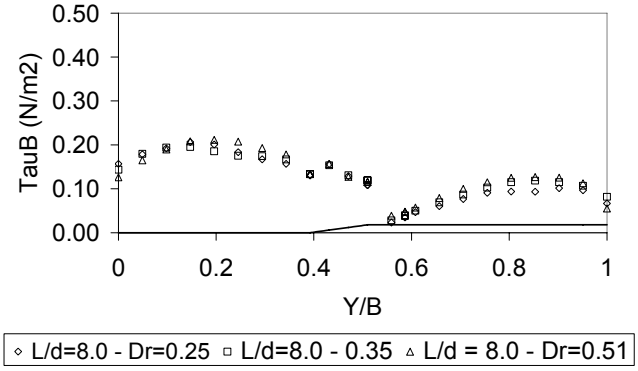

Figure 11. Boundary shear stress distribution for the brush cases with L/d=8 (Cases B8)

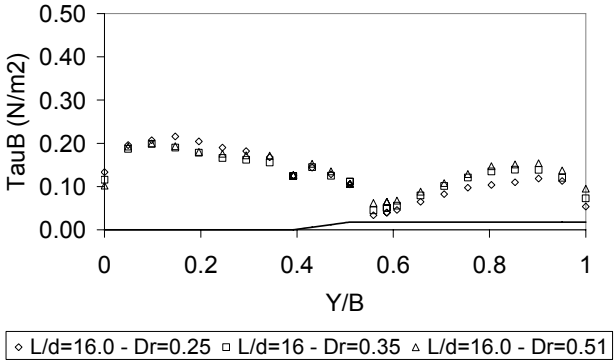

Figure 12. Boundary shear stress distribution for the brush cases with L/d=16 (Cases B16)

The reduction in boundary shear stress compared to the no rod case increases with relative depth. This reduction varies between 30.6% and 52.3% for cases B8a and B8c respectively and 27.3% and 54.9% for cases B16a and B16c respectively.

3.4 *Apparent shear stress*

A depth-averaged apparent shear stress τ_a is defined following Shiono and Knight (1991)'s definition (Equation 3).

$$\tau_a(y) = \frac{1}{H}\int_0^y \left[\rho g H S_0 - \tau_B\left(1-\frac{1}{s^2}\right)\right] dy \qquad (3)$$

Equation 3 can be solved provided boundary conditions are given. In this study, we assume that the depth-averaged apparent shear stress at y = 0 is equal to the left mean wall shear stress $\tau_{left\ wall}$ (Equation 4). Similarly, the depth averaged apparent shear stress at y = B is taken as the opposite of the right mean wall shear stress $\tau_{right\ wall}$ (Equation 5).

$$\tau_a(0) = \tau_{left\ wall} \qquad (4)$$

$$\tau_a(B) = -\tau_{right\ wall} \qquad (5)$$

The lateral variations of τ_a are presented in Figures 13 to 15.

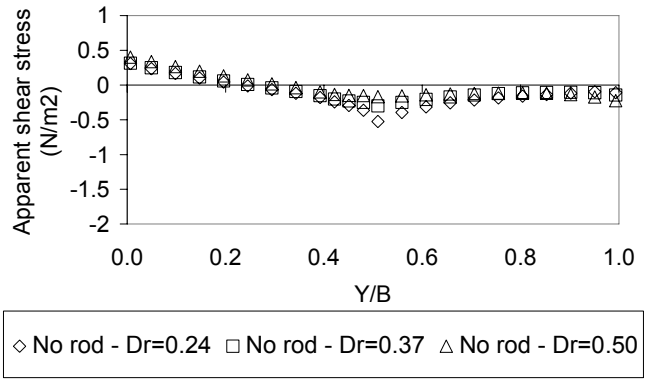

Figure 13. Apparent shear stress distribution for the no rod cases

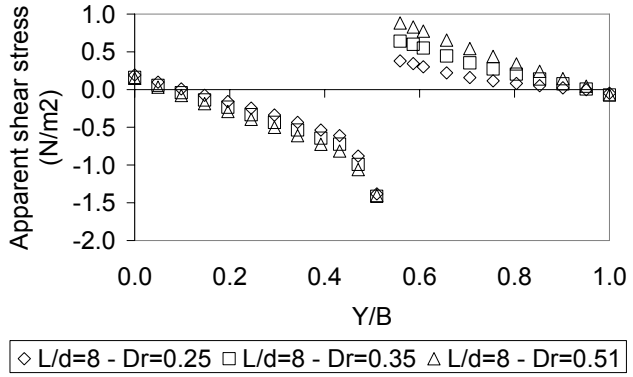

Figure 14. Apparent shear stress distribution for the with L/d=8 (Cases B8)

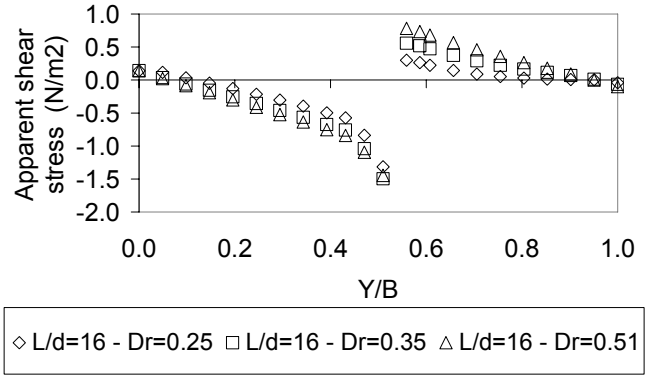

Figure 15. Apparent shear stress distribution for the with L/d=16 (Cases B16)

The brushes completely modify the distribution of apparent shear stress compared to the no rod case. The brushes have for clear impact to increase the amplitude of apparent shear stress either side of the vegetated interface. For each spacing ratio, the apparent shear stress remains similar in the main channel although one notes a slight decrease when relative depth increases. On the other hand, the apparent shear stress increases remarkably with relative depth in the floodplain.

3.5 *Drag force*

The total drag force per unit length in the channel can be calculated by force balance using Equation 6.

$$F_D = W_G - \int_0^B \tau_B(y)dy \tag{6}$$

The results of drag force calculations for the brush cases using the force balance approach are presented in Figure 16. It has been shown that as the water depth increases, the boundary shear force changes very little. However, drag force increases very rapidly as the water depth, and hence the weight component, increases for both vegetative densities.

As seen in Figure 16, the drag force varies almost linearly with relative water for both rod densities.

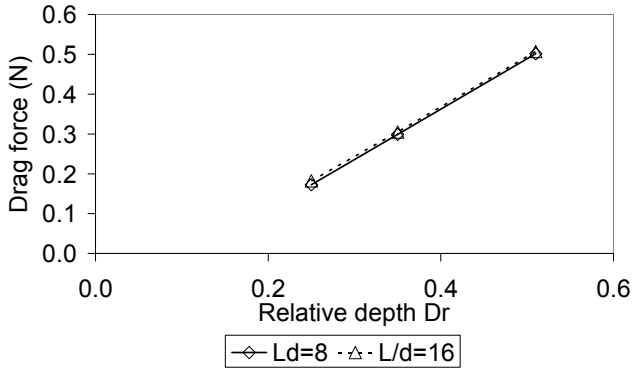

Figure 16. Drag force derived from force balance for the brush cases

The drag force can also be determined via the analytical formulae presented in Equation 7.

$$F_D = \frac{1}{2}\rho C_D A_P U^2 \tag{7}$$

Where C_D is the drag coefficient, A_P is the projected area and U is taken as the mean depth-averaged velocity across the section. In order to obtain the drag coefficient corresponding to the drag force per unit length derived from force balance, F_D is divided by the distance L between two brushes. The results are presented in Figure 17 against relative depth.

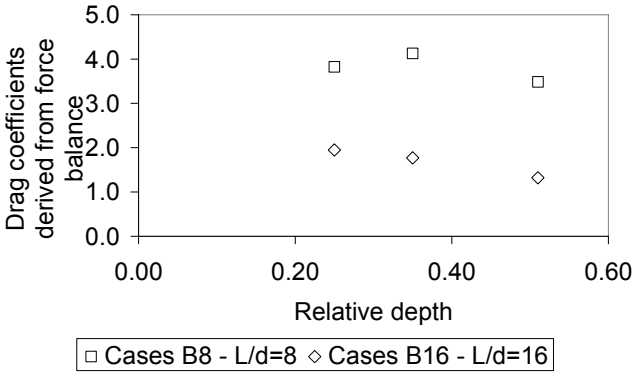

Figure 17. Variation of drag coefficients derived from force balance method against relative depth

The drag coefficients derived from force balance are typically greater than one and vary between 1.32 and 4.13, the highest drag coefficients being obtained for the denser case. The discrepancy between the drag coefficients of cases B8 and B16 increases with relative depth.

In literature, drag coefficients are also found to be derived from references taken for a unique cylinder and related to the rod Reynolds number Re_{rod} (Equation 7), such as in Schlichting and Gersten (1968).

$$\mathrm{Re}_{rod} = \frac{UD}{\nu} \tag{7}$$

Where ν is the kinematic viscosity. Drag coefficients derived for a unique cylinder from the rod Reynolds numbers remain close to unity for all cases.

4 DISCUSSION

The experiments highlighted a clear change in the velocity and boundary shear stress distribution due to the line of brushes placed on the edge of floodplain. These results have similarities with those presented by Sun and Shiono (2009), where experiments were carried out with a line of smooth wooden rods on the edge of floodplain. Both depth-averaged velocity and boundary shear stress profiles "dive" in the rod area, as they are reduced.

Perhaps the most striking result of these experiments lies in the increased channel discharge with increased density. It had first been expected that an increase in the brush density would lead to a decreased flow capacity in the channel. However, these results suggest a more complicated relationship between stage, discharge and vegetation density. It can be inferred that there is a threshold at which a closer spacing of brushes can result in an increase in discharge.

The drag coefficients calculated from force balance method are all greater than one. These results correlate the results from Jarvela (2004), who investigated the drag of non submerged leafless woody vegetation and who advocates the use of drag coefficients greater than 1 to account for the branch structure. The drag coefficients presented in this paper are also to be related to those presented in James *et al.* (2008), where the values of the plant drag coefficient for a single reed stem with different degrees of foliage were studied. The plant drag coefficients increased from approximately 5.4 for a stem with 6 leaves to 7.5 for a stem with full foliage for the range of vegetative Reynolds number investigated. The results suggest that adopting a drag coefficient from rod Reynolds number would underestimate drag force.

5 CONCLUSIONS

Experiments were carried out in a straight compound channel at Loughborough University for three relative depths. Two sets of experiments had lines of rods with bristles spaced out at rod distance to diameter ratios of L/d=8 and L/d=16. Velocity and boundary shear stress were measured with a Pitot tube and a Preston tube respectively. The results were compared to corresponding no rod cases.

Inspection of the stage-discharge curves shows that increasing vegetative density in the case of brushes can lead to an increase in the total channel discharge. This suggests that, although increasing vegetative density can lead to an increase in the chances of flooding, there is also a point at which closer spacing of brushes can result in an increase in discharge, thereby reducing flooding effects. This depends on foliage density. It is therefore important to consider how the vegetative density and discharge relate to flow depth when planting trees instead of simply increasing the spacing ratio with the aim of reducing the cumulative drag effects.

The flow reduction increases with relative depth and reaches approximately 50% when compared to the no rod. In the main channel, the maximum depth averaged velocity is pushed closer to the boundary wall with increasing flow depth, which correlates the results of Sun and Shiono (2009).

The lateral distributions of boundary shear stress follow closely the distributions of depth-averaged velocity. On the floodplain, boundary shear stress increases with relative depth with the maximum moving closer to the boundary wall with smaller relative depths, as was the case with the depth averaged velocity distributions.

The boundary shear stress is strongly reduced compared to the corresponding no rod cases as drag contributes to flow resistance. The reduction in boundary shear stress varies between 30.6% and 52.3% for cases B8a and B8c respectively and 27.3% and 54.9% for cases B16a and B16c respectively.

In the brush cases, the amplitude of apparent shear stress either side of the line of the interface is increased compared to the no rod case. For each spacing ratio, the apparent shear stress remains similar in the main channel. However, the apparent shear stress increases remarkably with relative depth in the floodplain.

Drag force per unit width can be calculated by force balance, by subtracting the boundary shear stress integrated over the wetted perimeter to the corresponding weight component. The results show a linear variation of drag force for both spacing ratios.

The drag coefficients calculated from the analytical formulae and deducted from the above drag force values were all greater than 1 and reached 4.13. This is significantly greater than the values of drag coefficients for a unique cylinder derived from rod Reynolds numbers, which all remain close to unity.

ACKNOWLEDGMENT

The first and second authors wish to thank the Civil and Building Engineering Department of Loughborough for sponsoring this research. The support of the PMI2 British Council is also acknowledged.

REFERENCES

Heanen, A., Myers, W. and Lyness, J. 2004. The conveyance capacity of compound channels with large scale floodplain roughness. In River Flow 2004, Napoli, Italy, 459-468.

Hubble, T., Docker, B. and Rutherfurd, I. 2009. The role of riparian trees in maintaining riverbank stability: A review of australian experience and practice. Ecological Engineering, Article in Press.

Igarashi, T. 1984. Characteristics of the flow around two circular cylinders arranged in tandem. Bulletin of Japanese Society of Mechanical Engineers, 27, 2380-2387;

James, C., Goldbeck, U., Patini, A. And Jordanova, A. 2008. Influence of foliage on flow resistance of emergent vegetation. Journal of Hydraulic Research, 46, 536-542;

Jarvela, J., 2004. Determination of flow resistance caused by non-submerged woody vegetation. International Journal of River Basin Management, 2, 61-70;

Nepf, H.M. 1999. Drag, turbulence, and diffusion in flow through emergent vegetation. Water Resources Research, 35(2), 479–489;

Pasche, E., Rouve, G. Overbank flow with vegetatively roughened flood plains 1985. Journal of Hydraulic Engineering, 111(9), 1262–1278.

Patel, V.C. 1965. Calibration of preston tube and limitations on its use in pressure gradients. Journal of Fluid Mechanics, 23, 185–208;

Patel, V.C. 1965. Calibration of preston tube and limitations on its use in pressure gradients. Journal of Fluid Mechanics, 23, 185–208;

Schlichting, H., Gersten, K. 1968. Boundary Layer Theory, 6th Edition. McGraw-Hill, New York;

Sun, X., Shiono, K. 2009. Flow resistance of one-line emergent vegetation along the floodplain edge of a compound open channel. Advances in Water Resources, 32, 430-438;

Terrier, B. 2010. Flow Characteristics in Straight Compound Channels with Vegetation along the Main Channel. PhD Thesis, Loughborough University;

Zdravkovitch, M. 1977. Review of flow interference between two circular cylinders in various arrangements. Journal of Fluids Engineering - Transactions of the ASME, 99, 618-633.